Advanced Algorithms in Medical Computer Graphics

Jan Klein[1], Dirk Bartz[2], Ola Friman[1], Markus Hadwiger[3], Bernhard Preim[4], Felix Ritter[1], Anna Vilanova[5], Gabriel Zachmann[6]

[1]MeVis Research, Germany
[2]University of Leipzig, Visual Computing (ICCAS), Germany
[3]VRVis Research Center, Vienna, Austria
[4]Otto-von-Guericke-University, Institute for Simulation and Graphics, Germany
[5]Eindhoven University of Technology, Department of Biomedical Engineering, Netherlands
[6]TU Clausthal, Department of Informatics, Germany

Abstract
Advanced algorithms and efficient visualization techniques are of major importance in intra-operative imaging and image-guided surgery. The surgical environment is characterized by a high information flow and fast decisions, requiring efficient and intuitive presentation of complex medical data and precision in the visualization results. Regions or organs that are classified as risk structures are in this context of particular interest. This paper summarizes advanced algorithms for medical visualization with special focus on risk structures such as tumors, vascular systems and white matter fiber tracts. Algorithms and techniques employed in intra-operative situations or virtual and mixed reality simulations are discussed. Finally, the prototyping and software development process of medical visualization algorithms is addressed.

Categories and Subject Descriptors (according to ACM CCS): I.3.5 [Computer Graphics]: Computational Geometry and Object-Modeling I.3.7 [Computer Graphics]: Three-Dimensional Graphics and Realism I.4.0 [Image Processing and Computer Vision]: General J.3 [Computer Applications]: Life and Medical Science

1. Introduction

Surgical intervention planning and clinical diagnostic systems benefit from the large variety of imaging modalities and visualization tools currently available. The Computed Tomography (CT) technology is developing rapidly with so-called dual source scanners already available and 256-row detectors soon on the market. With these scanners one can, for example, acquire high resolution image volumes covering the entire human heart with voxel sizes below 0.5 mm in less than 100 ms. Magnetic Resonance Imaging (MRI) scanners evolve at the same pace towards stronger magnetic fields and improved hardware. Apart from being able to acquire conventional high-resolution anatomical images with excellent contrast between soft tissue types, the flexible MRI technique is increasingly being used to depict functional information, such as cortical activation with functional MRI and blood flow with phase-contrast MRI, as well as specialized anatomical information such as major white matter tracts using diffusion tensor imaging (DTI). The imaging technology development has spawned a corresponding de-velopment of algorithms for analyzing, visualizing and combining the wealth of data produced, see Figure 1.

This state-of-the-art report summarizes advanced medical visualization and processing algorithms and puts them into the clinical context, including intra-operative solutions, image-guided surgery and virtual and augmented reality. The visualization algorithms may be categorized based on their input data (scalars, vectors, tensors):

Scalar Data

Volume rendering algorithms (Section 2.1) constitute the basis for visualizing raw 3D medical data. They offer overview presentations of scalar volumetric data from CT or MR scans without prior segmentation of specific regions or organs of interest such as bones or vessels (Section 2.2). In the context of volume rendering we consider the problem of inter-active performance with very large medical data volumes as well as the problem of finding an appropriate transfer function which maps the scalar data values to optical properties. Moreover, the visualization of vascular systems from scalar
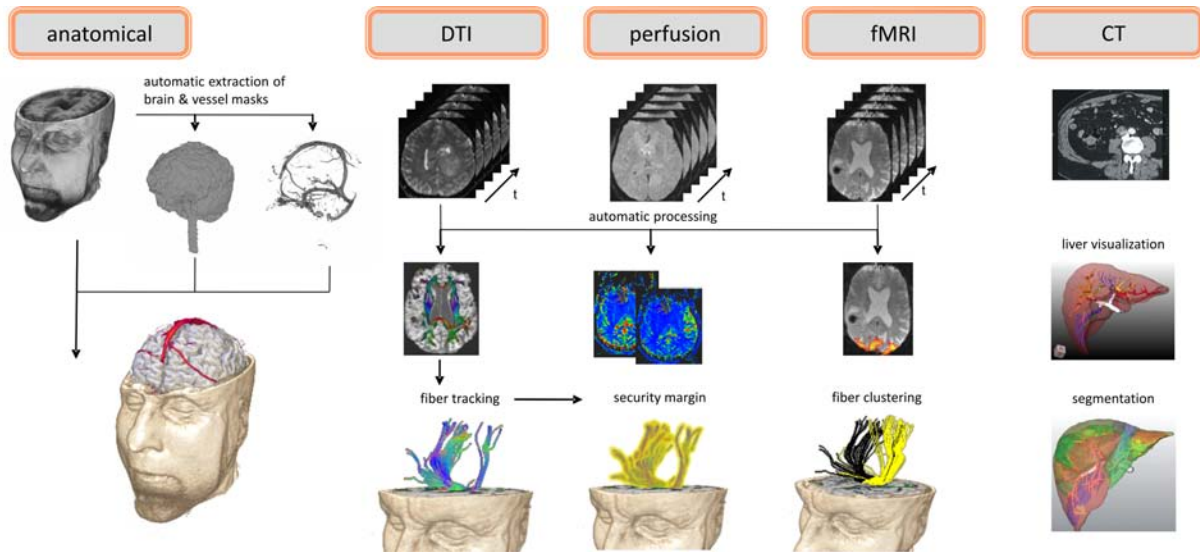
Figure 1: *Different visualization algorithms like volume rendering, maximum intensity projection, isosurface rendering and diffusion tensor imaging techniques can be used to process the multimodal image data in a useful way.*

data is considered, with a focus on modeling to convey shape and topology.

Vector and Tensor Data

Vector data and tensor data are produced by phase-contrast MRI [WEF*99] and diffusion weighted MRI [BMB94]. Phase-contrast MRI measures blood flow and generates 3D+Time velocity vector fields that need to be visualized in a judicious way. Diffusion weighted MRI measures water diffusion and the data is commonly projected on a tensor model for visualizing diffusion anisotropy. The anisotropy reflects the underlying tissue structure, e.g., of the heart muscle or white matter fiber tracts. Similar to the case of vascular structures, the visualization should provide knowledge about the location, properties, spatial distances, and functional relationships between fibers.

In Section 2.3, a short introduction to diffusion tensor MRI data will be presented. The techniques employed for visualizing the complex tensor data, as well as current challenges, will be explained. These techniques range from simplification to scalar information, glyph visualization and so-called fiber tracking. In addition, we also review fiber clustering methods that aim to extract structures with higher semantic meaning than a fiber or a tensor.

Image-guided Surgery, Virtual and Augmented Reality

The major challenge here is to link the pre-operative data sets with the patient on the operation table. To this end, we consider registration techniques, passive optical tracking as well as electromagnetic field tracking (Section 3.1). Moreover, intra-operative imaging techniques which re-scan the patient in the operation room (Section 3.2), as well as virtual and augmented reality methods that add context information from the present situation, are reviewed (Section 3.3). Collision detection algorithms are an essential component in image-guided surgery and virtual reality applications. Such algorithms are considered in Section 3.4.

Prototyping and Software Development

Finally, in Section 4 the needs and issues in the development of medical visualization algorithms are addressed. We focus on rapid prototyping software platforms which allow an evolutionary software development where ideas and requests of clinicians are easily integrated.

2. Visualization

2.1. Volume Rendering

Direct volume rendering (DVR) is the most common way of depicting scalar volumetric data such as CT or MR scans in their entirety, instead of extracting surfaces corresponding to specific objects of interest (e.g., bones, vessels), or looking at a collection of individual slice images, which is still common in radiology.

The volume is thought of as a collection of particles with certain physical properties that describe their interaction with light, e.g., absorption, emission, and scattering of light, which are subsumed in an *optical model* [Max95].

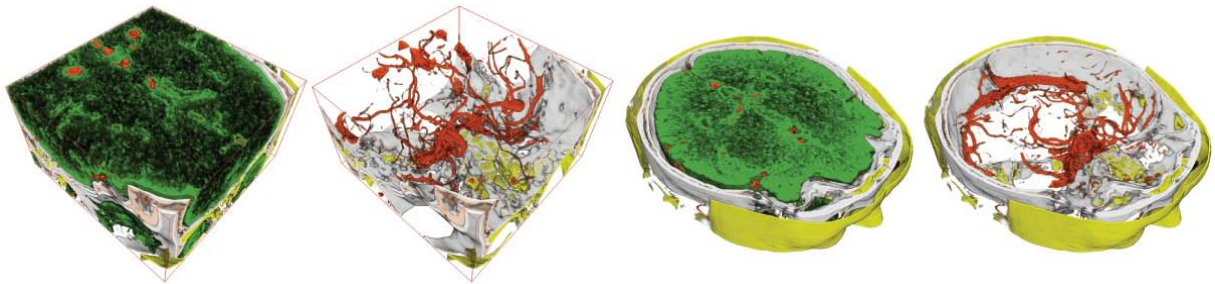In order to obtain an image of the entire volume, the

Figure 2: *Examples of a semantic transfer function model for CT angiography, with the anatomical structures brain, soft tissue, bone, and vasculature [RSKK06]. Transfer functions are not specified directly, but via structures' names and visual attributes.*

volume rendering integral corresponding to a chosen optical model is solved along viewing rays from the eye point through pixels of the output image plane [EHK*06]. This integral is usually solved via discretization, where individual samples are taken, mapped to optical properties, and combined in order to obtain an approximate result of sufficient quality [EHK*06], essentially performing Riemann integration.

In the medical context, interactive performance is crucial, and the most common methods are CPU-based ray-casting [GBKG04], using dedicated hardware such as the VolumePro [PHK*99], and exploiting GPUs (graphics processing units) either with texture slicing [RSEB*00], or ray-casting, which has only become possible in recent years [KW03, SSK*05, KSS*05]. Alternative approaches are *shear-warp* [MH01] and *splatting* [NM05], which is especially suited to visualizing sparsely populated volumes such as vasculature [VHHFG05].

A fundamental practical problem has always been the significant size of medical volume data, which is usually tackled via bricking approaches [LHJ99, KMM*01], which can also be used in conjunction with single-pass ray-casting in order to remove the per-brick setup overhead [HSS*05]. Recent GPU ray-casting implementations employing bricking are able to render volumes with several thousand slices [LWP*06], which can also use an out-of-core approach in order to avoid loading the entire volume into CPU memory. A basic operation that most bricking approaches employ is culling bricks against the transfer function in order to determine fully transparent bricks that can be neglected during rendering [GBKG04].

Current high-end GPUs are available with memory sizes from 512MB to 2GB, which enables rendering relatively large volumes even without bricking. However, further practical restrictions in addition to overall memory size are limits of maximum texture dimension (number of texels/voxels along each axis) and the ability to allocate huge 3D textures in one piece, instead of allocating multiple smaller textures. Both of these restrictions can be circumvented by bricking.

Naturally, when multiple imaging modalities and thus multiple volumes are visualized concurrently, memory requirements increase further, which can also be tackled with bricking strategies [BHWB07].

Interactive volume rendering has been restricted to orthogonal projection for a long time. However, recent advances in GPU-based ray-casting easily allow for perspective projection, which is especially important in virtual endoscopy [SHNB06]. In contrast to texture slicing, ray-casting also increases flexibility, such as allowing adaptive sampling rates [RGW*03], and in general is much easier to implement [EHK*06].

Incorporating ray-casting into an application for surgery planning and training allows one, for example, to change the isovalue corresponding to the surface of the colon or a vessel interactively for virtual endoscopy [NWF*05], also displaying background objects on demand, or using full DVR for the background [SHNB06].

A major issue in direct volume rendering is how scalar data values are mapped to optical properties, which is commonly done via a global *transfer function*. Powerful transfer function domains, i.e., the spaces in which they are specified, can be used in real-time volume rendering [KKH01, KPI*03]. However, specification of transfer functions is still a major hurdle for physicians, who are often using presets and easily overwhelmed by the complexity of transfer functions and the time required to specify them, especially when 2D or higher-dimensional transfer functions are used.

Recent advances such as *semantic transfer functions* [RSKK06, RBG07] can improve usability drastically, which has the potential for significantly increasing the acceptance of volume rendering by medical doctors in the future. Figure 2 shows visualizations generated using a semantic transfer function model that completely hides the underlying 2D transfer function domain from the user.

Another important issue is how to handle reliability or, vice versa, the *uncertainty*, that is inherent in visualizations. A recent approach in the context of medical appli-
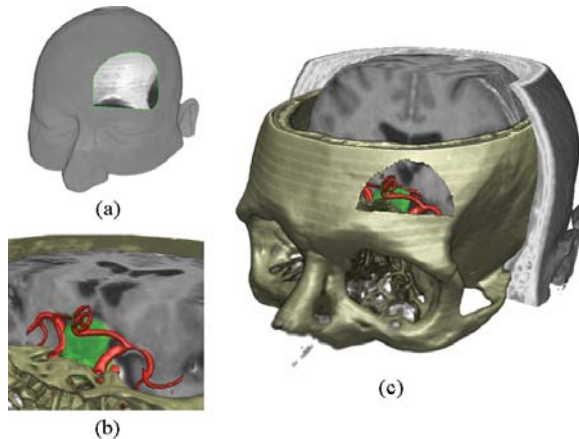
Figure 3: *Planning of a right subfrontal approach for pituitary tumor resection [BHWB07]. (a) Skin incision. (b) Operating microscope view. (c) Keyhole approach planning. Single-pass ray-casting can combine multiple modalities in real-time: MRI (skin and brain); CT (bone); MRA (vessels).*

cations tackles this issue using probabilistic animation, in order to visually convey the uncertainty in the classification that results from applying a probabilisitic transfer function [LLPY07].

Both incorporating domain knowledge and domain-specific conventions and metaphors, e.g., semantic approaches, as well as visualizing error and uncertainty have been identified as important research challenges for the future by the NIH-NSF Visualization Research Challenges Report [JMM*06].

If a transfer function alone does not suffice in order to separate different objects (tissues, organs) of interest, *segmentation* becomes necessary, which incorporates spatial information into the volume rendering process by specifying which object each voxel belongs to. Segmentation information can be used in real-time volume rendering to allow for per-object transfer functions or rendering modes [HBH03], and also provides a powerful basis for multi-volume rendering in which multiple modalities such as CT, MRI, fMRI, and PET are combined on a per-object basis using per-modality and per-object transfer functions [BHWB07]. Figure 3 shows three stages of an application for preoperative planning of a neurosurgical keyhole approach.

Analogously to transfer function specification, visualizing the uncertainty in segmentation results allows to better assess the risk involved in using the resulting visualizations [KVS*05].

One possibility to circumvent both, transfer function specification and segmentation, is to use *opacity peeling* [RSK06], which removes occluding parts of the volume in a view-dependent manner, which can also be modified to

exploit co-registered CT and MR volumes in order to improve reliability when viewing the brain without segmentation [BHWB07].

2.2. Vessel Visualization

Understanding the branching pattern and topology of vascular structures is crucial for therapy planning and the actual surgery in order to prevent healthy organs or organ regions from being cut off from blood supply and drainage. A 3D visualization that provides knowledge about the location, properties, spatial distances, and functional relationships of those vessels to other relevant anatomic structures has been a frequent request by surgeons. While current therapy planning software can provide most of this information, an integrated visualization that enables the surgeon to make reliable judgments without time-consuming, interactive inspections still remains an open request. During surgery, the surgeon has even less time to analyze complex visualizations than at the planning stage. Ideally, such visualization would therefore be static in a sense of facilitating frequent look-ups of required information yet providing all necessary morphological and spatial information in one single picture. Such a picture could be printed, displayed on a monitor inside the operation theater, and eventually projected on the very organ before dissection. The perception of spatial distances, however, becomes demanding when viewing a static, monoscopic projection of a 3D visualization. This is especially true for complex vascular systems that may consist of multiple interweaved tree-like structures such as the vascular systems of the liver (portal vein, liver artery, hepatic veins, and biliary duct). The effectiveness and lucidity of the visualization highly depend on the accentuation of spatial depth as well as the perceptive separation of important, individual properties. To improve the communication of both aspects, the real-time vascular visualization methods presented in this paper utilize and extend on illustrative rendering techniques that provide functional realism [Fer01]. Illustrative visualization methods not only allow us to emphasize or omit properties, but also offer visualization techniques with limited use of color. Due to varying absorption and reflection characteristics on organ surfaces, the perceived color and brightness gradations resulting from a traditional shaded projection on the organ are difficult to predict, thus making them less suited for this purpose. Instead we propose the use of texture as an alternative visual attribute. This allows us to encode additional information, such as the local distance to a tumor.

For the diagnosis of vascular diseases, 2D as well as conventional 3D visualization techniques, such as direct volume rendering, maximum intensity projection and isosurface rendering, are employed. With these methods, the underlying image data are faithfully represented [TKS*04]. However, artifacts due to inhomogeneity of contrast agent distribution and aliasing problems due to the limited spatial resolution
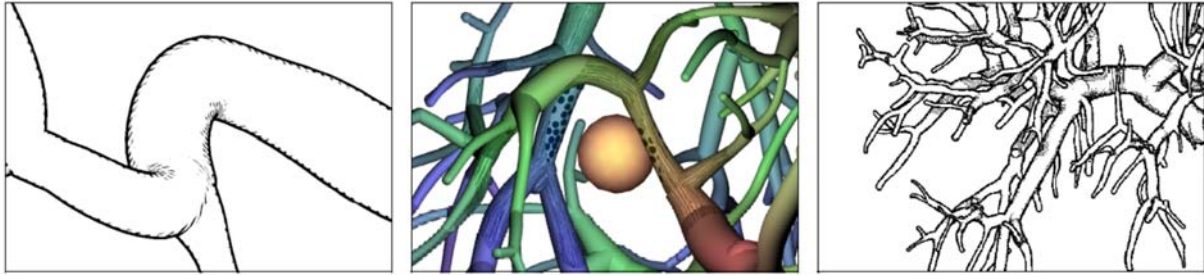
Figure 4: *Examples of vascular illustrations enhancing perception of properties important in surgery. Left and right image: Hatching indicates curvature and distances; middle image: Textures indicate distances to a generalized lesion (orange).*

may hamper the interpretation of spatial relations. Therefore, explicit surface reconstructions of vascular structures are often preferred for surgical therapy planning and intra-operative visualization, where the interpretation of vascular connectivity and topology is more important than the visualization of vascular diseases [BHH*05].

The idea of model-based reconstruction has been introduced by Gerig et al. [GKS*93]. A variety of further reconstruction methods have been developed which use the skeleton of a vascular tree and the local radius information as input. Assuming a circular cross section, surfaces of vascular trees are either explicitly constructed or implicitly created by means of an implicit description. Among the explicit methods, graphics primitives such as cylinders [MMD96] and truncated cones [HPSP01] are employed. A general problem of these methods are discontinuities, which primarily occur at branchings. The overcome such problems, smooth transitions can be modeled by freeform surfaces [EDKS94]. The most advanced explicit reconstruction technique is based on subdivision surfaces [FWB04]. An initial base mesh is constructed along the vessel centerline. The base mesh consists of quadrilateral patches and can be subdivided and refined according to the Catmull- Clark scheme.

Implicit modeling is used in general to achieve smooth and organic shapes. A special variant, convolution surfaces, can be used to represent skeletal structures [BS91]. With careful selection of a convolution filter, this concept allows to faithfully represent the local diameter of vascular structures [OP05]. A comprehensive survey of methods for vessel analysis and visualization is given in [BFC04].

Algorithms which aim at improving spatial perception, particularly depth perception, and at communicating important vascular properties by using and extending illustrative visualization techniques have been proposed in [RHD*06], see Figure 4.

2.3. Diffusion Tensor Imaging

In the last decade the new imaging modality diffusion tensor imaging (DTI) [BMB94] has generated new challenges and

a need for new developments in image analysis and visualization [VZKL06].

resonance (MR) imaging modality that allows the measurement of water diffusion in tissue. The water molecules in tissue with an oriented structure, e.g., the white matter in the brain, tend to diffuse along the structure. The diffusion process is generally modeled by a Gaussian probability density function, or equivalently, it is described by a second order tensor (i.e., a symmetric 3×3 matrix whose eigenvalues are real and positive). It is assumed that the diffusion tensor reflects the underlying tissue structure, for example, that the main eigenvector points out the main orientation.

Applications

DTI was initially developed for visualizing white matter in the brain but its use has later been extended to include for example tumor dissection [HJ02, SDGH*04] and investigations of ischemic muscle tissue in the heart [HMM*98, HSV*05, PVSH06]. Specifically, after infarction the fiber structure of the heart muscle is remodeled to adapt to the new conditions. Changes in the fiber structure can be measured with DTI, with the aim of understanding why the fiber remodeling sometimes fails, leading to a collapse of the heart. Yet another interesting application is the use of DTI for preterm neonates or neonates who suffer from hypoxic ischemia [PBV*06]. Being able to detect possible damages in the brain at an early stage yields the possibility to initiate a therapy that ensures the best possible development of the child. For all these applications, advanced visualization plays a crucial role, since the raw DTI data acquired by the MR scanner do not lend itself to visual inspection.

Visualizing the Tensors

The most common DTI visualization technique used in clinical environments is based on a scalar valued function of the tensor, i.e., the information in the 6 independent variables in the 3×3 symmetric tensor is reduced to one scalar that represents some relevant characteristic, mainly anisotropy (e.g., fractional anisotropy, relative
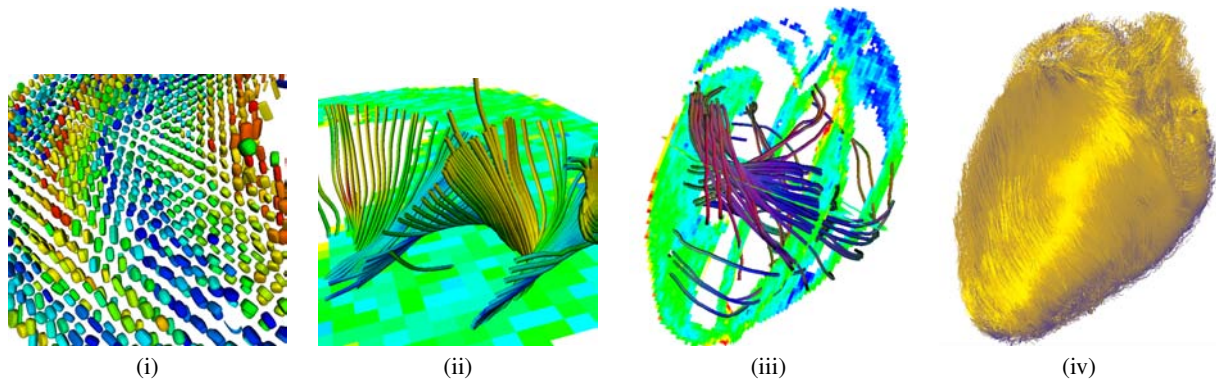
Figure 5: *Different visualizations of a healthy mouse heart data set with resolution 128x128x64: (i) superquadrics glyph in a region of the heart using hue color coding of the helix angle (ii) limited length fiber tracks obtain with seeding in a radial line. It shows the local helix form (iii) fiber tracking with region seeding. Fibers shown as tubes and color coded according to main eigenvector. Cross sections showing hue color map of the fractional anisotropy (iv) fiber tracking with full volume seeding and using illuminated streamlines*

anisotropy) [BP96]. The resulting scalar data can be visualized using common scalar field visualization techniques; from 2D cutting plane color mappings to volume rendering or even surface information that may reveal anatomically relevant information [KWH00].

When visualizing intrinsic 6D data as scalars, information is inevitably lost. In the case of diffusion tensors, diffusion shape and orientation cannot be conveyed in maps of diffusion anisotropy. Another group of techniques use glyph representations to visualize the tensor data, see Figure 5(i). Several glyph shapes have been used, i.e., ellipsoids, cuboids, and superquadrics [Kin04]. These methods are able to show the full tensor data without any information reduction. However, the clinical value of this visualization technique remains an open question as a human may have difficulties perceiving relevant information. Although techniques have been proposed to improve the perception by optimizing the placement of glyphs [KW06], cluttering is still a problem.

Fiber Tracking

Fiber tracking techniques aim at reconstructing the fibrous tissue structure from the diffusion tensor information. The advantage of these methods is that the result is analogous to what the physicians or radiologists are expecting and an extensive amount of research has therefore been focussed on this reconstruction [BPP*00, MZ02, WKL99]. The fiber tracking techniques can be divided into three categories:

- Streamline tracking
- Geodesic tracking
- Probabilistic tracking

In the streamline algorithms, the tensor field is reduced to a vector field consisting of the main eigenvectors of the ten-

sors. This vector field can then be visualized using common techniques in flow visualization. An extension to streamlines are streamsurfaces, where a surface represented by the two main eigenvectors is reconstructed in areas of planar anisotropy [ZDL03, VBP04]. The disadvantage of the streamline methods is that they do not make full use of tensor information and thresholds based on anisotropy indices are required to define when the main eigenvector is valid. Another disadvantage is that the results are dependent on the seeding strategy for the streamlines. Often the seeding regions are defined manually by the user and therefore are biased. Furthermore, relevant information can be missed with unfortunately chosen seed points.

The geodesic tracking methods define a new metric based on the diffusion tensors [OHW02, PWKB02]. This metric is generally based on the inverse of the diffusion tensor so that two points are close two each other if a path of high diffusion connecting the points exists. Tracking can then be performed by calculating geodesic paths in this new metric. These approaches do not discard tensor information and they are for this reason believed to be more robust. The main disadvantage is the computational complexity and the fact that there is always a geodesic between two points in the space. Hence, to separate geodesics following the underlying fibrous structure from invalid ones, there is not only the need to define seed points but also end points or connectivity measures.

The probabilistic tracking methods aim to visualizing the uncertainty present in DTI data by incorporating models of the acquisition process and noise [BBKW02, LAG*06, FFW06]. The uncertainty is assessed by tracking many possible paths originating from a single seed point and in this process taking the tensor uncertainty into account. Based on the tracked paths, maps of connectivity probabilities are pro-
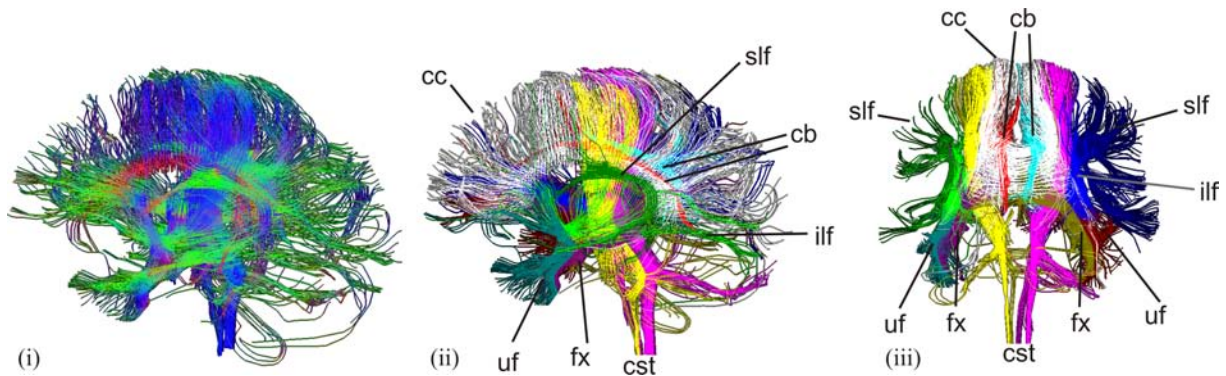
Figure 6: *(i) Fiber tracts colored corresponding to their local direction. (ii) and (iii) The visualization of clustered fiber tracts improves the perception and allows for a better interaction with the data, e.g., single bundles can be selected for quantification processes (cc=corpus callosum, slf=superior longitudinal fasciculus, cb=cingulum bundle, ilf=inferior longitudinal fasciculus, cst=cortico-spinal tract, fx=fornix, uf=uncinate fasciculus).*

duced, see Figure 7. Such maps may be used to delineate risk structures for pre-surgical planning.

Fiber Clustering

To avoid user-biased results or missing information due to subjective streamline seeding, one strategy is to seed the whole domain using 3D seeding strategies [VBP04]. However, the result is usually very cluttered and gives few insights in the data (see Figure 6(i)), even if computer graphics techniques are applied to improve the perception, see Figure 5(iv) [PVSH06]. It has been proposed to improve the interaction such that manual selection of the interesting fiber structures is done in a intuitive and reproducible way [ZDK*01, ASM*04, BBP*05]. Although these methods improve the inspection of the data, the resulting selections remain biased by the user.

In practice, the interesting structures are not individual fibers, which in any case are impossible to reconstruct since the DTI resolution is much lower than the diameter of the individual fibers. Instead, the interesting structures are anatomical meaningful bundles that fibers form. Furthermore, it is interesting to compare individuals or groups of individuals, e.g., patients and normal controls, and quantify similarities and differences.

Fiber clustering algorithms [DGA03, BKP*04, KBL*07, JHTW05, MMH*05, OKS*06, MVvW05] have been developed to group anatomically similar or related fibers into bundles (see Figure 6(ii) and 6(iii)) . As no user interaction is needed, undesirable bias is excluded. One of the main questions in several of this algorithms is when are two fibers considered to be similar or related forming a bundle. Different distance/similarity measures between fibers can be defined (e.g., Hausdorf distance, mean distance [MVvW05]). Furthermore, there are a large bunch of clustering techniques

that can be used and this have several parameters that need to be adjusted. One of the issues in this field is which of these techniques or which combination of them would give the best result. This is not a trivial questions and validation is an active and important field of research in DTI. Moberts et al. [MVvW05] did a first attempt to define a framework where the clustering techniques can be validated.

A group of clustering algorithms map the high-dimensional fiber data to a low dimensional feature space from which an affinity matrix is calculated [BKP*04]. In these techniques, the similarity is assumed to appear from the data itself. This calculation as well as the subsequent clustering needs $O(n^2)$ time, which means the running time is quadratic in the number of fibers. Especially if an automatic clustering of all available fibers is needed, this high running time is undesirable. The necessary adjustment of several parameters of the feature space, which often influences the number and the constellation of clusters in an unpredictable way, as well as the imprecise approximation by a feature space becomes obsolete by using a fiber grid [KBL*07] or voxel grid [JHTW05]. However, the actual clustering step remains in $O(n^2)$. The problem of an imprecise approximation can also be solved by a B-spline representation of fibers [MMH*05] where an efficient matching between B-splines can be performed [CHY95]. Alternatively, fibers can be represented very precisely and efficiently by parameterized polynomials defining the *x*-, *y*-, and *z*-components of the fiber points individually [KSS*08]. Based on that representation, a two-step clustering method allows to determine clusters in linear time $O(n)$ [KSS*08].

The fiber clustering algorithms are initialized with the results of a fiber tracking algorithm and therefore there is a transformation of the original data before the clustering is taking place. Unfortunately, the clustering results are also
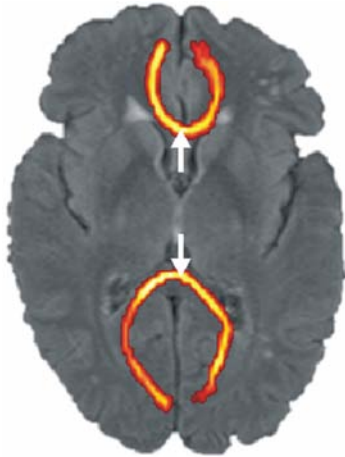
Figure 7: *Brain connectivity maps generated by tracking a large number of traces from the points indicated by the arrows. Such maps can be used to delineate risk structures, in this case the Corpus Callosum in the brain. The white arrows indicate the seed points used for starting the tracking process.*

depend on the fiber tracking technique used. To avoid this dependency you might obtain the anatomical bundles by directly segmenting the tensor field. Some recent work have shown the results of extending existing segmentation techniques into tensor fields [ZMB*03, JBH*05, WV05]. Similar to the clustering algorithms one of the main questions is how do you decide when two tensors are similar or belong to the same region. This is a complex question since it is not obvious in tensor fields what is the distance or difference between to tensors. In literature, there are several distance/similarity measures between tensors that have been proposed [AGB99, AFPA06]. However, it is a challenge to define the right measure for a given problem. Furthermore, current algorithms for tensor field segmentation are very time consuming. Interactivity is however necessary to be able to define and tune the segmentations.

As we mentioned, no much information can be extracted directly from the DTI raw data. Therefore, it is very important that image analysis and visualization techniques that help the understanding of this data are reliable. Validation of the DTI algorithms reminds a big challenge, since there is no trivial way to generate a ground truth and comparison method for DTI data. Furthermore, presenting the DTI data to a user in a comprehensive way where there is a balance between data simplification and clarity of the visualization remains an important issue. In a lot of applications physicians or radiologists want to distinguish between healthy and pathology, or evaluate changes on time, in an objective way. Finding good quantitative non biased ways to evaluate dif-

ferences, as well as, visualization and navigation tools that help identify these differences are also of major importance for the clinical application of DTI.

3. Image-guided Surgery and Virtual Reality for Medicine

One classic vision in surgery is to enable the surgeon with an "x-ray view" that allows her/him to inspect interior regions of the body that are hidden behind other organs. Virtual reality – or actually augmented reality – techniques are addressing exactly that approach by enriching ("augmenting") the traditional view on the patient with virtual information of the hidden regions. Of particular interest are the regions or organs that are classified as risk structures, like vascular structures (Section 2.2) or white matter fiber tracts (Section 2.3), because they are vital and must not be damaged during the surgical intervention, or because the organ is the specific target of the intervention.

3.1. Image-guided Surgery

Information on these structures of interest can be acquired by a pre-operative scan of the patient, typically done by a CT or MRI scanner. While this is already common practice in diagnosis and surgery planning (see Section 2.3), the major issue here is how to connect the pre-operative dataset(s) with the patient on the operation room (OR)-table. The basic solution for that issue is to register the dataset to the patient, or actually the OR-table to which the patient is fixed. This process requires the association of landmarks visible in the dataset and on the patient. While a minimum of four such associations is needed, typically six or more associations are established to improve accuracy and stability of the registration. Unfortunately, anatomical landmarks can vary significantly and are sometimes very difficult and tedious to identify. Instead, artificial markers, fiducials - which are easy to locate in the dataset and on the patient - are attached to the patient before the pre-operative scan.

After establishing the geometric transformation between the dataset and OR-table, the virtual data from the dataset can be related to the patient, providing the patient is not moved independently from the OR-table.

The position and orientation (or pose) of the OR-table is measured on basis of a reference array – which is a defined, identifiable object – that in turn is measured by a tracking system. While a number of different techniques are available, passive optical tracking based on infrared light and cameras is the currently most widely used technique. Here, one (or more) infrared light sources emit infrared light that is reflected by spherical markers of the reference array and again captured by two cameras mounted in a fixed geometric relationship. The position of that marker is then computed by triangulating the information of the reflection of the marker by both cameras. In order to compute also the orientation of
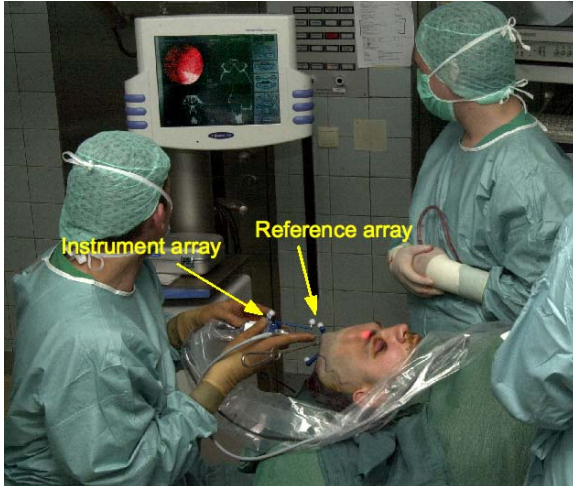
Figure 8: *Tracking of a surgical screw driver through an instrument array.*

Figure 9: *Multimodal representation of cerebral ventricular system and local vascular architecture from two MRI datasets, from an endoscopic point of view. The blue ellipsoid shows the arterial Circle of Willis.*

the reference array, a minimum of three reflective markers in a constant geometric relationship is needed. Since the cameras always see only projections of the markers, the accuracy of the computed position depends on the geometric arrangement of the markers; the more linearly independent they are, the better.

Similarly, tools (e.g., pointers. endoscopes, probes, etc.) are tracked through another marker array (instrument array) by the tracking system (see Figure 8). A different geometric configuration (number of markers, distance and angles between the markers) allows the identification of the respective tool and - even more important - the differentiation from the OR-table reference array.

Alternatively to optical infrared tracking, electromagnetic field tracking also becomes more popular recently. While it has clear advantages, since it does not require a fixed relationship between tooltip and reference markers and also no optical visibility of the markers, it is subject of various electro-magnetic field measuring artifacts if ferromagnetic or metal objects are introduced into the magnetic field. For this reason, we will not further describe this approach here, more details can be found in [PB07].

The combined system of marker/sensor arrays and tracking system is called in surgery intra-operative navigation system and largely defines the field of image-guided surgery.

Unfortunately, a number of caveats come with this approach. First, the accuracy depends largely on the diligence of the registration procedure. A sloppy registration will not ensure a sufficient overlap between dataset and patient. Second, several environmental factors may introduce measurement inaccuracies which reduce the tracking quality. In particular optical infrared tracking is subject to scattered in-
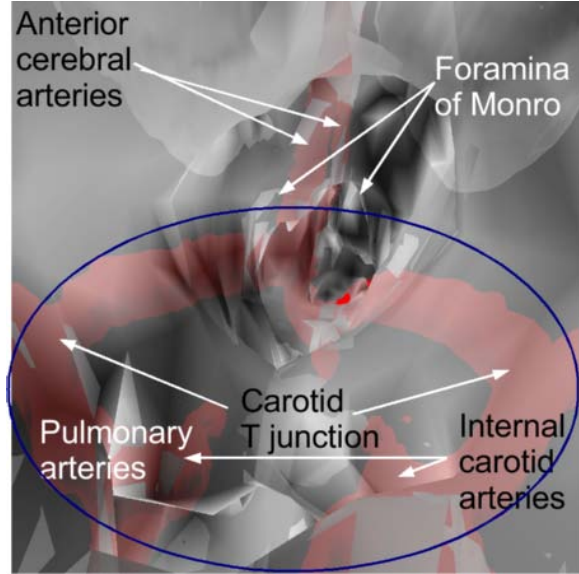
frared light from day light or physical deformations of the camera array during warm-up. Finally, the whole procedure builds on the assumption that the patient - or the actual target region of the patient - has not changed significantly since the pre-operative scan, hence the four to six associations are sufficient to describe the geometric relationship. If this assumption is not sufficiently valid, the whole registration procedure becomes dramatically more complex, because the body changes induce deformations of the datasets, possibly down to every voxel. Therefore, this situation requires elastic (non-rigid) registration with computational costs that are currently prohibitive for the surgical routine[†]. An overview of different registration techniques (rigid and non-rigid), can be found in [MV98].

3.2. Intra-operative Imaging

Alternatively to more advanced registration approaches, intra-operative imaging re-scans the patient on the OR-table. Any changes of the body with relevance to the scanning process are capture, depending on the scanning device. A typical example is the brain shift [LHNE99], where changes of pressure in the head after opening of the skull and of the dura (the leather-like hard skin of the brain) lead to position and

---

[†] Next to the computational costs, elastic registration also gives rise to questions how accurately the deformed dataset represents the reality.
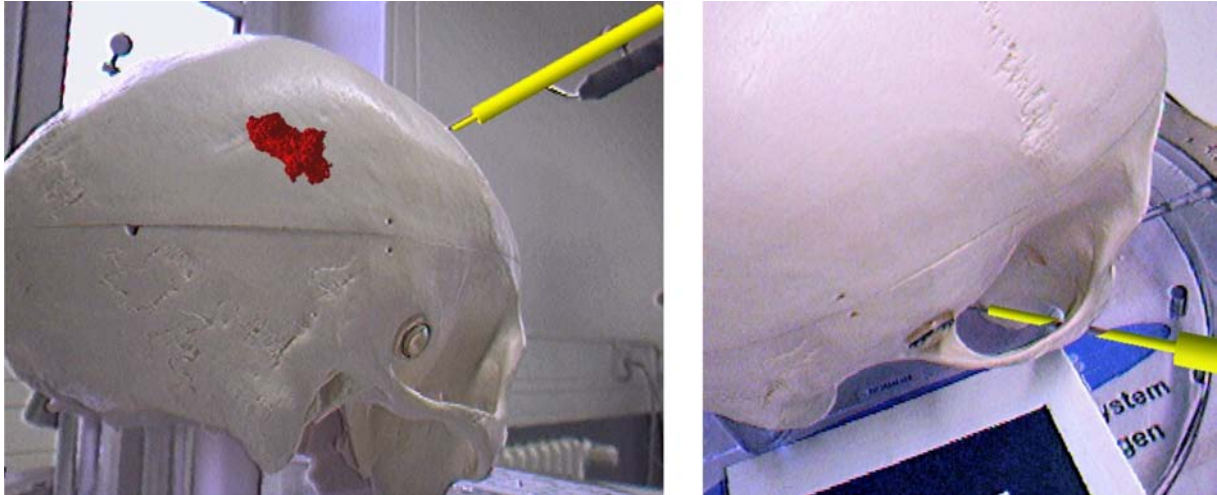
Figure 10: *Mixed reality display for a patient skull phantom. A virtual representation of a tumor (red) is augmented in the camera image (left). The virtual representation of the instrument (yellow) is augmented taking into account occlusion information. The occlusion information is correctly computed also for complex situations, where the cheek bone occludes the instrument (right).*

shape changes of the brain. The brain shift becomes even stronger after the (surgical) removal of tissue (e.g., tumor tissue) from the brain.

Note, however, that intra-operative scanning is a complex issue and typically requires a compromise on either image quality or costs. Intra-operative scanners are typically more mobile than pre-operative scanners, which often leads to simpler devices, and hence to a lower image quality. An example for this situation are pre- and intra-operative CT scanners. Intra-operative MRI scanners used to provide access for the surgeons to the patient, hence the name Open MR. Technical boundary conditions unfortunately allowed only a less powerful magnetic field ("low field") which provided only a significantly lower image quality. Recently, full field MRI scanners were introduced into the OR, providing an image quality comparable to regular pre-operative scanner [NGvKF03]. Unfortunately, intra-operative full field MRI requires numerous changes to the OR, rendering this method as a quite expensive one.

A good compromise represents intra-operative ultrasound, where a tracked ultrasound probe acquires 2D or 3D data in (near) real-time. Intra-operative ultrasound is well-established and a cost efficient scanning methods. On the downside, it has a significantly lower signal-to-noise ratio than CT or MRI and is more difficult to interpret. In many situations, however, it can be used as a valuable tool [LEHS02, LTA*05]. Other intra-operative scanning techniques include x-ray, surface scanners, etc. Except for x-ray, they are yet to be widely used or are still research prototypes.

3.3. Virtual and Mixed Reality

Virtual reality simulates the interaction with virtual objects, which – as the name suggests – do not physically exist. Such medical simulations allow to experience realistic patient situations without exposing patients to the risks inherent in the learning process and is adaptable to situations involving widely varying clinical content [BWW*07]. A specific virtual reality application in medicine is virtual endoscopy, where a virtual camera inspects body cavities in a representation acquired by a medical tomographic scanner. Since a previous state-of-the-art-report focussed already on virtual endoscopy [Bar05], we just direct the interested user to that paper.

Augmented – or mixed – reality adds context information from the reality, which is captured either by an optical see-through display (e.g., a head-mounted display [BFH*00] or semi-transparent display [SSW02]), or by a video see-through display (e.g., a camera [FNBF04]). The main task is now to combine the virtual 3D objects and the 2D video stream in a meaningful way (in the following, we limit ourself to video see-through, but the issues and solutions are similar for optical see-through). A survey on this discussion can be found in [Azu97].

The first step is to calibrate the reality-capturing camera with the virtuality representing dataset. Since the dataset is already registered to the OR-table, we need to do the same for the camera images from the video stream. Typically, a specific pattern is captured by the camera to derive position and orientation of that pattern [KB99]. If both are already known – e.g., they have been registered to the OR-table –

and if the camera itself is tracked by the navigation system through a reference marker, we can close the transformation loop and provide the transformation of the camera image to the dataset, and hence provide an augmented representation [FNBF04]. Approaches in a less clinical, more technical environment are described for ultrasound guided needle biopsy in Bajura et al.'s and State et al.'s classic papers [BFO92, SLH*96]. Specific mixed reality systems for liver surgery are discussed in [SSS*03, LEH*04, BBR*03], and mixed reality endoscopy systems in [DSGP00, BGF*02]. An interactive, mixed reality system for the semiautomatic transfer function design was suggested by del Río et al. [dRFK*05].

A different issue of augmented reality is known as the occlusion problem. This problem is based on the 3D nature of virtual objects and the lack of 3D information in the camera video stream. Consequently, the 3D objects can only be drawn over the camera video stream, resulting in the wrong depth sorting of the 3D objects in the augmented stream. If the virtual objects would move behind a real object represented by the camera stream, it would be still drawn ontop of it, disturbing the immersion of the user. Different approaches have been proposed to address this problem. Fischer et al. suggested to compute a shadow 3D representation of the occluding object that is only drawn in the z-buffer, and hence occludes the virtual object [FBS04]. This approach works well, if sufficient information is available of the occluding object, for example if the occluding object was scanned beforehand (e.g., a patient's body part, see Figure 10). Other's address the problem in case of static occlusion [BWRT96,FHFG99] and dynamic occlusion with static backgrounds [FNBF04].

3.4. Collision Detection

Collision detection is an essential component in image-guided surgery as well as in virtual and mixed reality applications. In such environments, collisions among deformable organs have to be detected and resolved. Furthermore, collisions between surgical tools and deformable tissue have to be processed. In the case of topological changes due to cutting, self-collisions of tissue can occur and have to be handled [TKH*05]. As an interactive behavior of the surgery simulation is essential, efficient algorithms for collision detection are required.

There are several different approaches to the collision detection process. Bounding volume hierarchies (BVHs) have proven to be very efficient for rigid objects [Hub96, PG95, GLM96, KHM*98, Zac98, Zac02, AdBG*01, vdB97, LAM01, KGL*98, EL01]. In addition, they are a very powerful tool if dealing with reduced deformable models [JP04].

In contrast to the object-partitioning methods, space-partitioning approaches are mainly used in case of deforming objects as they are independent of changes in the object's

Figure 11: *Example application of collision detection (intestine surgery simulation). The objects in this case are highly deformable. Both self-collisions and collisions between different objects must be detected and handled. (Screenshot courtesy L. Raghupathi, L. Grisoni, F. Faure, D. Marchall, M.-P. Cani, C. Chaillou [RGF*04].)*

topology. For the partitioning, an octree [BT95, KSTK98], a BSP tree [Mel00] or a voxel grid [Tur90, MPT99, GDO00, ZY00] can be used.

For scenarios where deformable objects have to be tested against rigid objects, e.g., between a surgical knife and a liver, distance fields are a very elegant and simple solution that also provides collision information like contact normals or penetration depths [FL01, VSC01, SPG03, FSG03]. A distance field specifies the minimum distance to a surface for all (discrete) points in the field. In the literature, different data structures have been proposed for representing distance fields, e.g., octrees, BSP trees, or uniform grids. The problem of uniform grids, the large memory consumption, can be alleviated by a hierarchical data structure called *adaptively sampled distance fields* [FPRJ00]. For the collision detection problem, special attention to the continuity between different levels of the tree has to be paid [BMF03].

Stochastic methods are very interesting for time-critical scenarios. They offer the possibility to balance the quality of the collision detection against computation time, e.g., by selecting random pairs of colliding features as a guess of the potentially intersecting regions [RCFC03]. To identify the colliding regions when objects move or deform, temporal as well as spatial coherence can be exploited [LC92]. This stochastic approach, which was improved by [KNF04], can be applied to several collision detection problems [GD02, DDCB01]. [GD04] presented a Monte-Carlo based technique for collision detection. Samples are randomly generated on every object in order to discover interesting new regions. Then, the objects are efficiently tested for collision
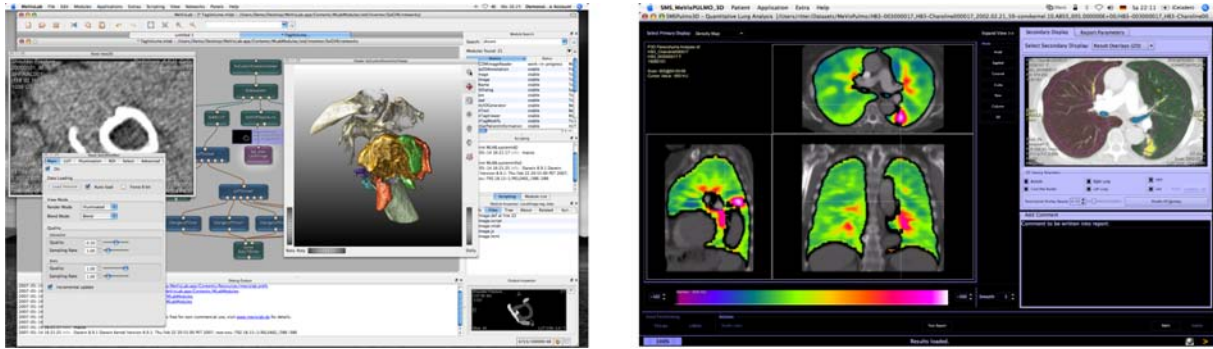
Figure 12: *Left: Module-based software development. Visualization algorithms are encapsulated by the green boxes. Right: Lung visualization (Pulmo-3D) which has been developed on top of MeVisLab.*

using a multiresolution layered shell representation, which is locally fitted according to the distance of the objects.

Hardware-assisted approaches, especially full GPU implementations, are a relatively novel technique. Their power, increasing faster than Moore's Law, and several new features are very interesting architectures to utilize for the collision detection [SF91, MOK95, LCN99, BW03, GZ03, GLM04] and/or self-collision detection [BW02, GLM03].

All mentioned collision detection algorithms provide some solutions for collision detection in medical applications. However, *the* most general, best-suited approach for all situations does not exist. If collisions between rigid and deformable objects have to be tested, as in the case of intra-operative situations, distance fields may be very useful. In applications where a real-time response is most important, such as training simulations and other virtual reality applications, stochastic approaches or GPU-based implementations could be preferable, which may incur some inaccuracy occasionally. If accuracy is of the utmost importance, then BVH based approaches are probably the most suitable choice.

Current challenges in collision detection are

- deformable objects (still), because it is notoriously difficult to find any acceleration data structures that can be updated quickly enough to be of any benefit;
- theoretical results about the average running time of the algorithms;
- stochastic collision detection is still an area that has received very little attention; and,
- collision detection on the recent multi-core architectures, such as the Cell processor or NVidia's Tesla architecture.

4. Prototyping and Integrating Algorithms in Medical Environments

Software development is associated with time and costs. In clinical environments and for algorithm evaluation in research settings, software that supports efficient visualization

of image data is required. However, the requirements differ in that clinical software should be easy to handle with few parameters to tune, whereas the research setting requires more elaborate testing scenarios. Furthermore, several application-independent generic issues must be addressed, such as data import and export of various medical image format standards (e.g. DICOM), user-management, reporting and documentation functionality. A substantial amount of development time must be invested to get these essential functions working. Nevertheless, new software systems are often built and maintained from scratch. A so-called application framework is a remedy that can be used to speed up the development process. Such a framework provides a reusable context that can be customized into specialized applications [FS97]. Ideally, components with common functionality are quickly connected to create a new product or prototype, while implementation details are encapsulated and hidden from the application developer. In this way, the development process is significantly shortened and the effort can be concentrated on the special requirements.

Various application framework tools have been developed to assist the design of clinical applications. Software platforms such as Analyze [RH90], SCIRun [JMPW04], VisiQuest [Vis07], or the LONI Pipeline Processing Environment [LON07] offer a rich set of algorithms for medical and scientific image analysis. Furthermore, image processing and visualization libraries such as ITK [ISNC05], VTK [SML97] and Open Inventor [Wer93] are available. MeVisLab [RKHP06] is an extendable framework for the development of software prototypes that focuses on medical applications for image-based diagnosis and therapy as well as for clinical research, see Figure 12. It offers a graphical programming interface where for example the functionality in ITK, VTK and Open Inventor is available as separate modules.

5. Conclusions

We have reviewed several algorithms for processing and visualizing medical image data, including scalar, vector and tensor data, with the aim of supporting image-guided surgery and mixed-reality simulations. The challenge when developing such algorithms is to extract relevant information and to present it in perceptible way, preferably at interactive speed. Recent advances in volume rendering techniques, like interactive rendering of perspective projections, GPU-based raycasting or semantic transfer functions, are able to handle the current sizes of medical data volumes and to present them to the clinician in an intuitive and useful way. However, interactive performance remains a problem.

Upcoming challenges include the visualization of multi-valued data. For example, patients are frequently examined with different medical imaging modalities and multi-modal visualization techniques that merge relevant information are for this reason an important research area. Moreover, vector valued and tensor valued data are gaining importance in the clinical environment. An example is the diffusion weighted MRI modality for which visualization of glyphs, fiber tracking and clustering are some of the processing techniques considered in this work.

In the context of vessel visualization, current challenges include the generation of geometric models appropriate for blood flow simulations. Preliminary results indicate that existing vessel visualization techniques may be adapted to produce meshes with sufficient triangle quality [SNB*08]. However, thorough investigations and comparisons with other techniques are necessary to come up with a reliable approach for visualizing vascular structures *and* simulating blood flow. With the information obtained via simulations, quantities such as wall shear stress which depend on morphologic, functional and dynamic factors may be investigated and visualized.

Finally, bringing the visualization algorithms from the research lab into the clinic and operation room is not only an engineering task. Intra-operative imaging data need to be registered with pre-operative data, augmented- and mixed-reality methods are still at their inception state and collision detection algorithms must be developed so that no bottlenecks arise when utilizing them in mixed-reality simulations. Rapid-prototyping and application frameworks are essential to implementing robust and user-friendly medical software and they facilitate the bridging between the clinical and research environments.

6. Biographies

Bartz, Dirk

Dirk Bartz is Associate Professor for Computer-Aided Surgery and directs the research group on Visual Computing at the ICCAS institute of the University of Leipzig. His recent works cover interactive visual medicine, perceptual graphics, illustrative and scientific visualization. In 2002, he received the NDI Young Investigator Award for his work on virtual endoscopy and intra-operative navigation. Dirk studied computer science and medicine at the University of Erlangen-Nürnberg and the Stony Brook University. He received a Diploma (M.Sc.) in computer science from the University of Erlangen-Nürnberg, a Ph.D. in computer science and a habitation in computer science from the University of Tübingen (all in Germany). His three most relevant publications in this context: [PB07, Bar05, FNBF04].

Friman, Ola

Ola Friman received the MSc degree in Electrical Engineering from Lund University, Sweden, in 1999, and the Ph.D. degree in Biomedical Engineering from Linköping University, Sweden, in 2003. His work on functional MRI was awarded with the Golden Mouse prize as the most prominent research project in Sweden 2001. During 2004-2005 he worked on diffusion tensor MRI at the Surgical Planning Laboratory, Brigham and Women's Hospital, Boston USA, and held Research Fellow and Instructor positions at Harvard Medical School. 2005 to 2006 he was working on Brain-Computer Interfaces and EEG signal processing at Bremen University, Germany. Dr. Friman is currently at MeVis Research, Germany. His research interests are signal processing, image processing, statistics and medical imaging. His three most relevant publications: [FFW06, PFJW06, FW05].

Hadwiger, Markus

Markus Hadwiger is a senior researcher at the VRVis Research Center in Vienna, Austria. He received his Ph.D. in computer science from the Vienna University of Technology in 2004, and has been a researcher at VRVis since 2000, working in the Basic Research on Visualization group and the Medical Visualization group (since 2004). He has been involved in several courses and tutorials on volume rendering and visualization at ACM SIGGRAPH, IEEE Visualization, and Eurographics. He is also a co-author of the book "Real-Time Volume Graphics" published by A K Peters. His three most relevant publications: [HSS*05, EHK*06, BHWB07].

Klein, Jan

Jan Klein is a senior researcher for neuroimaging at MeVis Research, Bremen, Germany with special focus on diffusion tensor imaging. He received his Ph.D. as well as his diploma (M.S.) in computer science from Paderborn University. Awards: prize of the faculty for one of the best Ph.D. theses in computer science (Paderborn University, 2006), Eurographics Medical Prize 2007 (first prize). His three most relevant publications: [KZ04a, KZ04b, HKN*06].

Preim, Bernhard

Bernhard Preim received his diploma in computer science in 1994 (minor in mathematics) and a Ph.D. in 1998 from

the Otto-von-Guericke University of Magdeburg. In June 2002 he received the Habilitation degree (venia legendi) for computer science from the University of Bremen. Since March 2003 he is a full professor for "Visualization" at the computer science department at the Otto-von-Guericke-University of Magdeburg, heading a research group which is focussed on medical visualization and applications in surgical education and surgical planning. These developments are summarized in a comprehensive textbook Visualization in Medicine (co-author Dirk Bartz), which appeared at Morgan Kaufman in April 2007. His three most relevant publications: [OP05, ODH*07, PB07].

Ritter, Felix
Felix Ritter is a senior researcher for visualization at MeVis Research, Bremen, Germany. His research interests are medical visualization, perception and human factors in visualization. His current work is focused on the usability of medical workstations, with respect to interaction and visualization of multimodal image data. He has authored and co-authored papers in the field of medical visualization and human computer interaction. He received a Ph.D. in Computer Science from the University of Magdeburg, Germany in 2005. His three most relevant publications [RDPS01, RSHS03, RHD*06].

Vilanova, Anna
Anna Vilanova is an assistant professor and head of a research group at the Biomedical Image Analysis group at the Biomedical Engineering department of the Eindhoven University of Technology. She received her Ph.D. degree in 2001 from the Vienna University of Technology. Her current research interests are medical visualization and image analysis. Her three most relevant publications: [MVvW05, VBP04, VZKL06].

Zachmann, Gabriel
Gabriel Zachmann is professor for computer graphics at Clausthal University, Germany, since 2005. Prior to that, he was assistant professor with Prof. Reinhard Klein's computer graphics group at Bonn University, Germany, and head of the research group for novel interaction methods in virtual prototyping. In 2000, Dr. Zachmann received a Ph.D. in computer science, and in 1994 a Dipl.-Inform (M.S.), both from Darmstadt University. He also studied computer science at Karlsruhe University. His three most relevant publications: [TKH*05, LZ06, Zac07].

References

[AdBG*01] AGARWAL P. K., DE BERG M., GUD-MUNDSSON J., HAMMAR M., HAVERKORT H. J.: Box-trees and r-trees with near-optimal query time. In *Proc. Seventeenth Annual Symposium on Computational Geometry (SCG 2001)* (2001), pp. 124–133.

[AFPA06] ARSIGNY V., FILLARD P., PENNEC X., AY-ACHE N.: Log-Euclidean metrics for fast and simple calculus on diffusion tensors. *Magnetic Resonance in Medicine 56*, 2 (August 2006), 411–421.

[AGB99] ALEXANDER D. C., GEE J. C., BAJCSY R.: Similarity measures for matching diffusion tensor images. In *BMVC* (1999).

[ASM*04] AKERS D., SHERBONDY A., MACKENZIE R., DOUGHERTY R., WANDELL B.: Exploration of the brain's white matter pathways with dynamic queries. In *IEEE Visualization* (October 2004), pp. 377–384.

[Azu97] AZUMA R.: A Survey of Augmented Reality. *Presence: Teleoperators and Virtual Environments 6*, 4 (1997), 355–385.

[Bar05] BARTZ D.: Virtual Endoscopy in Research and Clinical Practice. *Computer Graphics Forum 24*, 1 (2005), 111–126.

[BBKW02] BRUN A., BJÖRNEMO M., KIKINIS R., WESTIN C.-F.: White matter tractography using sequential importance sampling. In *Proceeding of ISMRM* (May 2002), p. 1131.

[BBP*05] BLAAS J., BOTHA C. P., PETERS B., VOS F., POST F. H.: Fast and reproducible fiber bundle selection in dti visualization. In *IEEE Visualization* (2005), pp. 59–64.

[BBR*03] BORNIK A., BEICHEL R., REITINGER B., GOTSCHULI G., SORANTIN E., LEBERL F., SONKA M.: Computer Aided Liver Surgery Planning Based on Augmented Reality Techniques. In *Proc. of Workshop Bildverarbeitung für die Medizin* (2003), Informatik Aktuell.

[BFC04] BÜHLER K., FELKEL P., CRUZ A. L.: Geometric methods for vessel visualization and quantification - a survey. In *Geometric Modeling for Scientific Visualization* (2004), Brunnet G., Hamann B., Müller H., (Eds.), Springer Verlag.

[BFH*00] BIRKFELLNER W., FIGL M., HUBER K., WATZINGER F., WANSCHITZ F., HANEL R., WAGNER A., RAFOLT D., EWERS R., BERGMANN H.: The Varioscope AR - A Head-Mounted Operating Microscope for Augmented Reality. In *Proc. of Medical Image Computing and Computer-Assisted Intervention (MICCAI)* (2000), Lecture Notes in Computer Science, pp. 869–877.

[BFO92] BAJURA M., FUCHS H., OHBUCHI R.: Merging Virtual Objects with the Real World: Seeing Ultrasound Imaginery within the Patient. In *Proc. of ACM SIGGRAPH* (1992), pp. 203–210.

[BGF*02] BARTZ D., GÜRVIT O., FREUDENSTEIN D., SCHIFFBAUER H., HOFFMANN J.: Integration von Navigation, optischer und virtueller Endoskopie in der Neuro- sowie Mund-, Kiefer- und Gesichtschirurgie. In *Jahrestagung der Deutschen Gesellschaft für Computer- und Roboterassistierte Chirurgie e.V. (CURAC)* (2002).

[BHH*05] BOSKAMP T., HAHN H., HINDENNACH M.,

ZIDOWITZ S., OELTZE S., PREIM B., PEITGEN H.-O.: Geometrical and structural analysis of vessel systems in 3d medical image datasets. *Medical Imaging Systems Technology 5* (2005), 1–60.

[BHWB07] BEYER J., HADWIGER M., WOLFSBERGER S., BÜHLER K.: High-quality multimodal volume rendering for preoperative planning of neurosurgical interventions. In *Proceedings of IEEE Visualization 2007* (2007), pp. 1696–1703.

[BKP*04] BRUN A., KNUTSSON H., PARK H. J., SHENTON M. E., WESTIN C.-F.: Clustering fiber tracts using normalized cuts. In *MICCAI'04* (2004), pp. 368–375.

[BMB94] BASSER P., MATTIELLO J., BIHAN D. L.: Mr diffusion tensor spectroscopy and imaging. *Biophysical Journal 66* (1994), 259–267.

[BMF03] BRIDSON R., MARINO S., FEDKIW R.: Simulation of clothing with folds and wrinkles. In *Proceedings of the 2003 ACM SIGGRAPH/Eurographics Symposium on Computer animation (SCA '03)* (2003), Eurographics Association, pp. 28–36.

[BP96] BASSER P., PIERPAOLI C.: Microstructural features measured using diffusion tensor imaging. *Journal of Magnetic Resonance* (1996), 209–219.

[BPP*00] BASSER P., PAJEVIC S., PIERPAOLI C., DUDA J., ALDROUBI A.: In vivo fiber tractography using dt-mri data. *Magn Reson Med. 44*, 4 (2000), 625–632.

[BS91] BLOOMENTHAL J., SHOEMAKE K.: Convolution surfaces. In *Proc. of ACM SIGGRAPH Conference on Computer Graphics* (1991), pp. 251–256.

[BT95] BANDI S., THALMANN D.: An adaptive spatial subdivision of the object space for fast collision detection of animating rigid bodies. *Computer Graphics Forum (Proc. of EUROGRAPHICS 1995) 14*, 3 (1995), 259–270.

[BW02] BACIU G., WONG W. S.-K.: Hardware-assisted self-collision for deformable surfaces. In *Proc. ACM Symposium on Virtual Reality Software and Technology (VRST 2002)* (Hong Kong, China, Nov. 2002), pp. 129–136.

[BW03] BACIU G., WONG W. S.-K.: Image-based techniques in a hybrid collision detector. *IEEE Transactions on Visualization and Computer Graphics 9*, 2 (2003), 254–271.

[BWRT96] BREEN D., WHITAKER R., ROSE E., TUCERYAN M.: Interactive Occlusion and Automatic Object Placement for Augmented Reality. *Computer Graphics Forum 15*, 3 (1996), 11–22.

[BWW*07] BINSTADT E., WALLS R., WHITE B., NADEL E., TAKAYESU J., BARKER T., NELSON S., POZNER C.: A comprehensive medical simulation education curriculum for emergency medicine residents. *Ann Emerg Med. 49*, 4 (2007), 495–504.

[CHY95] COHEN F. S., HUANG Z., YANG Z.: Invariant matching and identification of curves using b-splines curve representation. *IEEE Transactions on Image Processing 4*, 1 (1995), 1–10.

[DDCB01] DEBUNNE G., DESBRUN M., CANI M.-P., BARR A. H.: Dynamic real-time deformations using space and time adaptive sampling. *ACM Transactions on Graphics (SIGGRAPH 2001) 20*, 3 (2001), 31–36.

[DGA03] DING Z., GORE J. C., ANDERSON A. W.: Classification and quantification of neuronal fiber pathways using diffusion tensor MRI. *Magn. Reson. Med. 49* (2003), 716–721.

[dRFK*05] DEL RÍO A., FISCHER J., KÖBELE M., BARTZ D., STRASSER W.: Augmented Reality Interaction for Semiautomatic Volume Classification. In *Proc. of Eurographics Symposium on Virtual Environments* (2005), pp. 113–1320.

[DSGP00] DEY D., SLOMKA P. J., GOBBI D. G., PETERS T. M.: Mixed Reality Merging of Endoscopic Images and 3D Surfaces. In *Proc. of Medical Image Computing and Computer-Assisted Intervention (MICCAI)* (2000), Lecture Notes in Computer Science, pp. 796–803.

[EDKS94] EHRICKE H., DONNER K., KILLER W., STRASSER W.: Visualization of vasculature from volume data. *Computers and Graphics 18*, 3 (1994), 395–406.

[EHK*06] ENGEL K., HADWIGER M., KNISS J., REZK-SALAMA C., KNISS J.: *Real-Time Volume Graphics*. A K Peters, Ltd., 2006.

[EL01] EHMANN S. A., LIN M. C.: Accurate and fast proximity queries between polyhedra using convex surface decomposition. *Computer Graphics Forum (Proc. of EUROGRAPHICS 2001) 20*, 3 (2001), 500–510.

[FBS04] FISCHER J., BARTZ D., STRASSER W.: Occlusion Handling for Medical Augmented Reality Using a Volumetric Phantom Model. In *Proc. of ACM Symposium on Virtual Reality Software and Technology* (2004), pp. 174–177.

[Fer01] FERWERDA J.: Hi-fi rendering. In *Proc. of ACM Siggraph/Eurographics Campfire on Perceptually Adaptive Graphics* (2001).

[FFW06] FRIMAN O., FARNEBACK G., WESTIN C.-F.: A Bayesian approach for stochastic white matter tractography. *IEEE Transactions on Medical Imaging 25*, 8 (2006), 965–978.

[FHFG99] FUHRMANN A., HESINA G., FAURE F., GERVAUTZ M.: Occlusion in Collaborative Augmented Environments. *Computers & Graphics 23*, 6 (1999), 809–819.

[FL01] FISHER S., LIN M.: Fast penetration depth estimation for elastic bodies using deformed distance fields. In *Proc. International Conf. on Intelligent Robots and Systems (IROS)* (2001), pp. 330–336.

[FNBF04] FISCHER J., NEFF M., BARTZ D., FREUDEN-STEIN D.: Medical Augmented Reality based on Commercial Image Guided Surgery. In *Proc. of Eurographics Symposium on Virtual Environments* (2004), pp. 83–86.

[FPRJ00] FRISKEN S. P., PERRY R. N., ROCKWOOD A. P., JONES T. R.: Adaptively sampled distance fields: A general representation of shape for computer graphics. *ACM Transactions on Graphics (SIGGRAPH 2000) 19*, 3 (2000), 249–254.

[FS97] FAYAD M., SCHMIDT D. C.: Object-oriented application frameworks. *Commun. ACM 40*, 10 (1997), 32–38.

[FSG03] FUHRMANN A., SOBOTTKA G., GROSS C.: Distance fields for rapid collision detection in physically based modeling. In *Proceedings of GraphiCon 2003* (Moscow, Sept. 2003), pp. 58–65.

[FW05] FRIMAN O., WESTIN C.-F.: Uncertainty in white matter fiber tractography. In *MICCAI* (2005), pp. 107–114.

[FWB04] FELKEL P., WEGENKITTL R., BÜHLER K.: Surface models of tube trees. In *Computer Graphics International* (2004), pp. 70–77.

[GBKG04] GRIMM S., BRUCKNER S., KANITSAR A., GRÖLLER E.: Memory efficient acceleration structures and techniques for cpu-based volume raycasting of large data. In *Proceedings IEEE/SIGGRAPH Symposium on Volume Visualization and Graphics* (2004), pp. 1–8.

[GD02] GUY S., DEBUNNE G.: *Layered shells for fast collision detection*. Tech. rep., INRIA, 2002.

[GD04] GUY S., DEBUNNE G.: *Monte-Carlo collision detection*. Tech. Rep. RR-5136, INRIA, March 2004.

[GDO00] GANOVELLI F., DINGLIANA J., O'SULLIVAN C.: Buckettree: Improving collision detection between deformable objects. In *Proc. of Spring Conference in Computer Graphics (SCCG2000)* (Bratislava, 2000), pp. 156–163.

[GKS*93] GERIG G., KOLLER T., SZÉKELY G., BRECHBÜHLER C., KÜBLER O.: Symbolic description of 3-d structures applied to cerebral vessel tree obtained from mr angiography volume data. In *Proc. of Information Processing in Medical Imaging* (1993), vol. 687 of *Lecture Notes in Computer Science*, Springer, pp. 94–111.

[GLM96] GOTTSCHALK S., LIN M., MANOCHA D.: OBB-Tree: A hierarchical structure for rapid interference detection. *ACM Transactions on Graphics (SIGGRAPH 1996) 15*, 3 (1996), 171–180.

[GLM03] GOVINDARAJU N. K., LIN M. C., MANOCHA D.: *Fast Self-Collision Detection in General Environments using Graphics Processors*. Tech. Rep. TR03-044, University of North Carolina at Chapel Hill, 2003.

[GLM04] GOVINDARAJU N. K., LIN M. C., MANOCHA D.: Fast and reliable collision culling using graphics hardware. In *Symposium on Virtual Reality Software and Technology (VRST 2004)* (2004).

[GZ03] GRESS A., ZACHMANN G.: Object-space interference detection on programmable graphics hardware. In *SIAM Conf. on Geometric Design and Computing* (Seattle, Washington, Nov.13–17 2003).

[HBH03] HADWIGER M., BERGER C., HAUSER H.: High-quality two-level volume rendering of segmented data sets on consumer graphics hardware. In *Proceedings of IEEE Visualization 2003* (2003), pp. 301–308.

[HJ02] HORSFIELD M., JONES D.: Applications of diffusion-weighted and diffusion tensor MRI to white matter diseases – a review. *Nuclear Magnetic Resonance in Biomedicine 15*, 7-8 (2002), 570–577.

[HKN*06] HAHN H. K., KLEIN J., NIMSKY C., REXILIUS J., PEITGEN H.-O.: Uncertainty in diffusion tensor based fibre tracking. *Acta Neurochirurgica Supplementum 98* (2006), 33–41.

[HMM*98] HSU E., MUZIKANT A., MATULEVICIUS S., PENLAND R., HENRIQUEZ C.: Magnetic resonance myocardial fiber-orientation mapping with direct histological correlation. *Am J Physiology 274* (1998), 1627–1634.

[HPSP01] HAHN H. K., PREIM B., SELLE D., PEITGEN H.-O.: Visualization and interaction techniques for the exploration of vascular structures. In *Proc. of IEEE Visualization* (2001), pp. 395–402.

[HSS*05] HADWIGER M., SIGG C., SCHARSACH H., BUHLER K., GROSS M.: Real-time ray-casting and advanced shading of discrete isosurfaces. *Computer Graphics Forum 24*, 3 (2005), 303–312.

[HSV*05] HEEMSKERK A., STRIJKERS G., VILANOVA A., DROST M., NICOLAY K.: Determination of mouse skeletal muscle architecture using three dimensional diffusion tensor imaging. *Magn Reson Med. 53*, 6 (May 2005), 1333 – 1340.

[Hub96] HUBBARD P. M.: Approximating polyhedra with spheres for time-critical collision detection. *ACM Transactions on Graphics 15*, 3 (July 1996), 179–210.

[ISNC05] IBANEZ L., SCHROEDER W., NG L., CATES J.: *The ITK Software Guide*, second ed. Kitware, Inc. ISBN 1-930934-15-7, http://www.itk.org/ItkSoftwareGuide.pdf, 2005.

[JBH*05] JONASSON L., BRESSON X., HAGMANN P., CUISENAIRE O., MEULI R., THIRAN J.: White matter fiber tract segmentation in DT-MRI using geometric flows. *Medical Image Analysis 9*, 3 (June 2005), 223–236.

[JHTW05] JONASSON L., HAGMANN P., THIRAN J.-P., WEDEEN V. J.: Fiber tracts of high angular resolution dif-

fusion mri are easily segmented with spectral clustering. In *Proceeding of ISMRM* (2005), p. 1310.

[JMM*06] JOHNSON C. R., MOORHEAD R., MUNZNER T., PFISTER H., RHEINGANS P., YOO T. S. (Eds.): *NIH-NSF Visualization Research Challenges Report*. IEEE Press, Los Alamitos, CA, USA, 2006.

[JMPW04] JOHNSON C. R., MACLEOD R., PARKER S. G., WEINSTEIN D.: Biomedical computing and visualization software environments. *Commun. ACM 47*, 11 (2004), 64–71.

[JP04] JAMES D. L., PAI D. K.: BD-Tree: Output-sensitive collision detection for reduced deformable models. *ACM Transactions on Graphics (SIGGRAPH 2004) 23*, 3 (Aug. 2004), 393–398.

[KB99] KATO H., BILLINGHURST M.: Marker Tracking and HMD Calibration for a video-based Augmented Reality Conferencing System. In *Proc. of IEEE and ACM International Workshop on Augmented Reality* (1999), pp. 85–94.

[KBL*07] KLEIN J., BITTIHN P., LEDOCHOWITSCH P., HAHN H. K., KONRAD O., REXILIUS J., PEITGEN H.-O.: Grid-based spectral fiber clustering. *Proc. SPIE 6509* (2007). doi: 10.1117/12.706242.

[KGL*98] KRISHNAN S., GOPI M., LIN M. C., MANOCHA D., PATTEKAR A.: Rapid and accurate contact determination between spline models using Shell-Trees. *Computer Graphics Forum (Proc. of EURO-GRAPHICS 1998) 17*, 3 (Sept. 1998), 315–326.

[KHM*98] KLOSOWSKI J. T., HELD M., MITCHELL J. S. B., SOWRIZAL H., ZIKAN K.: Efficient collision detection using bounding volume hierarchies of *k*-DOPs. *IEEE Transactions on Visualization and Computer Graphics 4*, 1 (Jan. 1998), 21–36.

[Kin04] KINDLMANN G.: Superquadric tensor glyphs. In *Data Visualization (Proc. of Eurographics/IEEE Symposium on Visualization)* (May 2004), pp. 147–154.

[KKH01] KNISS J., KINDLMANN G., HANSEN C.: Interactive volume rendering using multi-dimensional transfer functions and direct manipulation widgets. In *Proceedings of IEEE Visualization 2001* (2001), pp. 255–262.

[KMM*01] KNISS J., MCCORMICK P., MCPHERSON A., AHRENS J., PAINTER J., KEAHEY A., HANSEN C.: Interactive texture-based volume rendering for large data sets. *IEEE Computer Graphics and Applications 21*, 4 (2001).

[KNF04] KIMMERLE S., NESME M., FAURE F.: Hierarchy accelerated stochastic collision detection. In *Proc. 9th International Fall Workshop Vision, Modeling, and Visualization (VMV 2004)* (2004).

[KPI*03] KNISS J., PREMOZE S., IKITS M., LEFOHN A., HANSEN C., PRAUN E.: Gaussian Transfer Functions for Multi-Field Volume Visualization. In *Proceedings of IEEE Visualization 2003* (2003), pp. 497–504.

[KSS*05] KLEIN T., STRENGERT M., STEGMAIER S., , ERTL T.: Exploiting frame-to-frame coherence for accelerating high-quality volume raycasting on graphics hardware. In *Proceedings of IEEE Visualization 2005* (2005), pp. 123–230.

[KSS*08] KLEIN J., STUKE H., STIELTJES B., KONRAD O., HAHN H. K., PEITGEN H.-O.: Efficient fiber clustering using parameterized polynomials. *Proc. SPIE, to appear* (2008).

[KSTK98] KITAMURA Y., SMITH A., TAKEMURA H., KISHINO F.: A real-time algorithm for accurate collision detection for deformable polyhedral objects. *Presence 7*, 1 (1998), 36–52.

[KVS*05] KNISS J., VAN UITERT R., STEPHENS A., LI G.-S., TASDIZEN T., HANSEN C.: Statistically Quantitative Volume Visualization. In *Proceedings of IEEE Visualization 2005* (2005), pp. 287–294.

[KW03] KRÜGER J., WESTERMANN R.: Acceleration techniques for gpu-based volume rendering. In *Proc. of IEEE Visualization 2003* (2003), pp. 287–292.

[KW06] KINDLMANN G., WESTIN C.-F.: Diffusion tensor visualization with glyph packing. *IEEE Transactions on Visualization and Computer Graphics 12*, 5 (September-October 2006), 1329–1336.

[KWH00] KINDLMANN G., WEINSTEIN D., HART D.: Strategies for direct volume rendering of diffusion tensor fields. *IEEE Transactions on Visualization and Computer Graphics 6*, 2 (2000), 124–138.

[KZ04a] KLEIN J., ZACHMANN G.: Point cloud collision detection. *Computer Graphics Forum (Proc. of Eurographics) 23*, 3 (2004), 567–576.

[KZ04b] KLEIN J., ZACHMANN G.: Point cloud surfaces using geometric proximity graphs. *Computers & Graphics 28*, 6 (2004), 839–850.

[LAG*06] LUA Y., ALDROUBIB A., GOREA J. C., ANDERSONA A., , DINGA Z.: Improved fiber tractography with bayesian tensor regularization. *NeuroImage 31*, 3 (2006), 1061–1074.

[LAM01] LARSSON T., AKENINE-MÖLLER T.: Collision detection for continuously deforming bodies. In *Eurographics* (2001), pp. 325–333. short presentation.

[LC92] LIN M. C., CANNY J. F.: Efficient collision detection for animation. In *Proc. of 3rd Eurographics Workshop on Animation and Simulation* (Cambridge, England, 1992).

[LCN99] LOMBARDO J.-C., CANI M.-P., NEYRET F.: Real-time collision detection for virtual surgery. In *Proc. of Computer Animation* (Geneva, Switzerland, May 1999), pp. 82–90.

[LEH*04] LANGE T., EULENSTEIN S., HÜNERBEIN M., LAMECKER H., SCHLAG P.-M.: Augmenting Intraoperative 3D Ultrasound with Preoperative Models for Navigation in Liver Surgery. In *Proc. of Medical Image Computing and Computer-Assisted Intervention (MICCAI)* (2004), vol. 3217 of *Lecture Notes in Computer Science*, pp. 534–541.

[LEHS02] LANGE T., EULENSTEIN S., HÜNERBEIN M., SCHLAG P.-M.: Vessel-Based Non-Rigid Registration of MR/CT and 3D Ultrasound for Navigation in Liver Surgery. *Computer Aided Surgery 8*, 5 (2002), 228–240.

[LHJ99] LAMAR E., HAMANN B., JOY K. I.: Multiresolution techniques for interactive texture-based volume visualization. In *IEEE Visualization* (1999), pp. 355–361.

[LHNE99] LÜRIG C., HASTREITER P., NIMSKY C., ERTL T.: Analysis and Visualization of the Brain Shift Phenomenon in Neurosurgery. In *Data Visualization (Proc. of Eurographics/IEEE Symposium on Visualization)* (1999), pp. 285–289.

[LLPY07] LUNDSTRÖM C., LJUNG P., PERSSON A., YNNERMAN A.: Uncertainty visualization in medical volume rendering using probabilistic animation. In *Proceedings of IEEE Visualization 2007* (2007), pp. 1648–1655.

[LON07] Laboratory of neuro imaging: Loni pipeline processing environment, http://www.loni.ucla.edu/Software/, 2007.

[LTA*05] LINDNER D., TRANTAKIS C., ARNOLD S., SCHMITGEN A., SCHNEIDER J., MEIXENSBERGER J.: Neuronavigation based on intraoperative 3D-Ultrasound during Tumor Resection. In *Proc. of Computer Assisted Radiology and Surgery* (2005), pp. 815–820.

[LWP*06] LJUNG P., WINSKOG C., PERSSON A., LUNDSTRÖM C., YNNERMAN A.: Full body virtual autopsies using a state-of-the-art volume rendering pipeline. In *Proceedings of IEEE Visualization 2006* (2006), pp. 869–876.

[LZ06] LANGETEPE E., ZACHMANN G.: *Geometric Data Structures for Computer Graphics*. A. K. Peters, Ltd., Natick, MA, USA, 2006.

[Max95] MAX N.: Optical models for direct volume rendering. *IEEE Transactions on Visualization and Computer Graphics 1*, 2 (1995), 99–108.

[Mel00] MELAX S.: Dynamic plane shifting bsp traversal. In *Graphics Interface 2000* (2000), pp. 213–220.

[MH01] MROZ L., HAUSER H.: Rtvr: a flexible java library for interactive volume rendering. In *Proceedings of IEEE Visualization 2001* (2001), pp. 279–286.

[MMD96] MASUTANI Y., MASAMUNE K., DOHI T.: Region-growing-based feature extraction algorithm for tree-like objects. *Visualization in Biomedical Computing 1131* (1996), 161–171.

[MMH*05] MADDAH M., MEWES A., HAKER S., GRIMSON W. E. L., WARFIELD S.: Automated atlas-based clustering of white matter fiber tracts from DTMRI. In *MICCAI'05* (2005), pp. 188–195.

[MOK95] MYSZKOWSKI K., OKUNEV O. G., KUNII T. L.: Fast collision detection between complex solids using rasterizing graphics hardware. *The Visual Computer 11*, 9 (1995), 497–512.

[MPT99] MCNEELY W. A., PUTERBAUGH K. D., TROY J. J.: Six degrees-of-freedom haptic rendering using voxel sampling. *ACM Transactions on Graphics (SIGGRAPH 1999) 18*, 3 (1999), 401–408.

[MV98] MAINTZ J., VIERGEVER M.: A Survey of Medical Image Registration. *Medical Image Analysis 2*, 1 (1998), 1–36.

[MVvW05] MOBERTS B., VILANOVA A., VAN WIJK J.: Evaluation of fiber clustering methods for diffusion tensor imaging. *IEEE Visualization* (2005), 65–72.

[MZ02] MORI S., ZIJL P. V.: Fiber tracking: principles and strategies – a technical review. *Nuclear Magnetic Resonance in Biomedicine 15*, 7-8 (2002), 468–480.

[NGvKF03] NIMSKY C., GANSLANDT O., VON KELLER B., FAHLBUSCH R.: Preliminary Experience in Glioma Surgery With Intraoperative High-Field MRI. *Acta Neurochirurgica 88* (2003), 21–29.

[NM05] NEOPHYTOU N., MUELLER K.: Gpu accelerated image aligned splatting. In *Proceedings of Volume Graphics 2005* (2005), pp. 197–205.

[NWF*05] NEUBAUER A., WOLFSBERGER S., FORSTER M.-T., MROZ L., WEGENKITTL R., BÜHLER K.: Advanced virtual endoscopic pituitary surgery. *IEEE Transactions on Visualization and Computer Graphics 11*, 5 (2005), 497–507.

[ODH*07] OELTZE S., DOLEISCH H., HAUSER H., MUIGG P., PREIM B.: Interactive visual analysis of perfusion data. *IEEE Transactions on Visualization and Computer Graphics* (2007).

[OHW02] O'DONNELL L., HAKER S., WESTIN C.: New approaches to estimation of white matter connectivity in diffusion tensor MRI: Elliptic PDE's and geodesics in tensor-warped space. In *Proc. of Medical Image Computing and Computer-Assisted Intervention (MICCAI)* (2002), pp. 459–466.

[OKS*06] O'DONNELL L., KUBICKI M., SHENTON M. E., DREUSICKE M., GRIMSON W. E. L., WESTIN C.-F.: A method for clustering white matter fiber tracts. *AJNR 27*, 5 (2006), 1032–1036.

[OP05] OELTZE S., PREIM B.: Visualization of vascular structures with convolution surfaces: Method, validation and evaluation. *IEEE Transactions on Medical Imaging 25*, 4 (2005), 540–549.

[PB07] PREIM B., BARTZ D.: *Visualization in Medicine - Theory, Algorithms, and Applications*. Morgan Kaufman Publishers, Burlington, 2007.

[PBV*06] PUL C., BUIJS J., VILANOVA A., ROOS F., WIJN P.: Fiber tracking in newborns with perinatal hypoxic-ischemia at birth and at 3 months. *Radiology 240*, 1 (2006), 203–214.

[PFJW06] PELED S., FRIMAN O., JOLESZ F., WESTIN C.-F.: Geometrically constrained two-tensor model for crossing tracts in DWI. *Magnetic Resonance Imaging 24*, 9 (2006), 1263–1270.

[PG95] PALMER I. J., GRIMSDALE R. L.: Collision detection for animation using sphere-trees. *Computer Graphics Forum 14*, 2 (June 1995), 105–116.

[PHK*99] PFISTER H., HARDENBERGH J., KNITTEL J., LAUER H., SEILER L.: The VolumePro real-time raycasting system. In *Proc. of SIGGRAPH '99* (1999), pp. 251–260.

[PVSH06] PEETERS T., VILANOVA A., STRIJKERS G., HAAR ROMENY B. T.: Visualization of the fibrous structure of the heart. In *Vision Modeling and Visualization-VMV 2006* (Nov 2006), pp. 309–317.

[PWKB02] PARKER G. J. M., WHEELER-KINGSHOTT C. A. M., BARKER G. J.: Estimating distributed anatomical connectivity using fast marching methods and diffusion tensor imaging. *IEEE Trans Med Imaging 21*, 5 (May 2002), 505–512.

[RBG07] RAUTEK P., BRUCKNER S., GRÖLLER M. E.: Semantic layers for illustrative volume rendering. In *Proceedings of IEEE Visualization 2007* (2007), pp. 1336–1343.

[RCFC03] RAGHUPATHI L., CANTIN V., FAURE F., CANI M.-P.: Real-time simulation of self-collisions for virtual intestinal surgery. In *Proceedings of the International Symposium on Surgery Simulation and Soft Tissue Modeling* (2003), Ayache N., Delingette H., (Eds.), no. 2673 in Lecture Notes in Computer Science, Springer-Verlag, pp. 15–26.

[RDPS01] RITTER F., DEUSSEN O., PREIM B., STROTHOTTE T.: Virtual 3d puzzles: A new method for exploring geometric models in vr. *IEEE Computer Graphics & Applications 21*, 5 (Sept./Oct. 2001), 11–13.

[RGF*04] RAGHUPATHI L., GRISONI L., FAURE F., MARCHALL D., CANI M.-P., CHAILLOU C.: An intestine surgery simulator: Real-time collision processing and visualization. *IEEE Transactions on Visualization and Computer Graphics (TVCG) 10*, 6 (Nov/Dec 2004), 708–718.

[RGW*03] RÖTTGER S., GUTHE S., WEISKOPF D., ERTL T., STRASSER W.: Smart hardware-accelerated volume rendering. In *Proceedings of VisSym 2003* (2003), pp. 231–238.

[RH90] ROBB R., HANSON D.: Analyze: A software system for biomedical image analysis. In *Proc. First Conf. Visualization in Biomedical Computing* (1990), pp. 507–518.

[RHD*06] RITTER F., HANSEN C., DICKEN V., KONRAD O., PREIM B., PEITGEN H.-O.: Real-Time Illustration of Vascular Structures. *IEEE Visualization 12*, 5 (2006), 877–884.

[RKHP06] REXILIUS J., KUHNIGK J.-M., HAHN H. K., PEITGEN H.-O.: An application framework for rapid prototyping of clinically applicable software assistants. In *GI Jahrestagung (1)* (2006), pp. 522–528.

[RSEB*00] REZK-SALAMA C., ENGEL K., BAUER M., GREINER G., ERTL T.: Interactive Volume Rendering on Standard PC Graphics Hardware Using Multi-Textures and Multi-Stage Rasterization. In *Proc. SIGGRAPH/Eurographics Workshop on Graphics Hardware* (2000).

[RSHS03] RITTER F., SONNET H., HARTMANN K., STROTHOTTE T.: Illustrative shadows: Integrating 3d and 2d information displays. In *Proc. of ACM Conference on Intelligent User Interfaces (Miami, Jan. 2003)* (2003), ACM Press, New York, pp. 166–173.

[RSK06] REZK-SALAMA C., KOLB A.: Opacity Peeling for Direct Volume Rendering. In *Computer Graphics Forum - Proc. of Eurographics* (2006), pp. 597–606.

[RSKK06] REZK-SALAMA C., KELLER M., KOHLMANN P.: High-level user interfaces for transfer function design with semantics. In *Proceedings of IEEE Visualization 2006* (2006), pp. 1021–1028.

[SDGH*04] SUNDGREN P., DONG Q., GOMEZ-HASSAN D., MUKHERJI S., MALY P., WELSH R.: Diffusion tensor imaging of the brain: review of clinical applications. *Neuroradiology 46*, 5 (2004), 339–350.

[SF91] SHINYA M., FORGUE M.-C.: Interference detection through rasterization. *The Journal of Visualization and Computer Animation 2*, 4 (Oct.–Dec. 1991), 132–134.

[SHNB06] SCHARSACH H., HADWIGER M., NEUBAUER A., BUHLER K.: Perspective isosurface and direct volume rendering for virtual endoscopy applications. In *Proceedings of Eurovis/IEEE-VGTC Symposium on Visualization* (2006), pp. 315–322.

[SLH*96] STATE A., LIVINGSTON M., HIROTA G., GARRETT W., WHITTON M., FUCHS H., PISANO E.: Technologies for Augmented-Reality Systems: Realizing Ultrasound-Guided Needle Biopsies. In *Proc. of ACM SIGGRAPH* (1996), pp. 439–446.

[SML97] SCHROEDER W., MARTIN K., LORENSEN B.: *The Visualization Toolkit: An Object-Oriented Approach to 3D Graphics*. Prentice Hall, 1997.

[SNB*08] SCHUMANN C., NEUGEBAUER M., BADE R.,

PEITGEN H.-O., PREIM B.: Implicit vessel surface reconstruction for visualization and cfd simulation. *International Journal of Computer Assisted Radiology and Surgery* (2008).

[SPG03] SIGG C., PEIKERT R., GROSS M.: Signed distance transform using graphics hardware. In *IEEE Vis2003* (2003), pp. 83–90.

[SSK*05] STEGMAIER S., STRENGERT M., KLEIN T., , ERTL T.: A simple and flexible volume rendering framework for graphics-hardware-based raycasting. In *Proceedings of Volume Graphics 2005* (2005), pp. 187–195.

[SSS*03] SCHEUERING M., SCHENK A., SCHNEIDER A., PREIM B., GREINER G.: Intra-operative Augmented Reality for Minimally Invasive Liver Interventions. In *Proc. of SPIE Medical Imaging* (2003), pp. 407–417.

[SSW02] SCHWALD B., SEIBERT H., WELLER T.: A Flexible Tracking Concept Applied to Medical Scenarios Using an AR Window. In *Proc. of IEEE and ACM International Symposium on Mixed and Augmented Reality* (2002), pp. 261–262.

[TKH*05] TESCHNER M., KIMMERLE S., HEIDELBERGER B., ZACHMANN G., RAGHUPATHI L., FUHRMANN A., CANI M.-P., FAURE F., MAGNENAT-THALMANN N., STRASSER W., VOLINO P.: Collision detection for deformable objects. *Computer Graphics forum 24*, 1 (Mar. 2005), 61–81.

[TKS*04] TOMANDL B. F., KÖSTNER N. C., SCHEMPERSHOFE M., HUK W. J., STRAUSS C., ANKER L., HASTREITER P.: Ct angiography of intracranial aneurysms: A focus on postprocessing. *Radiographics 24*, 3 (2004), 637–655.

[Tur90] TURK G.: *Interactive Collision Detection for Molecular Graphics*. Tech. Rep. TR90-014, University of North Carolina at Chapel Hill, 1990.

[VBP04] VILANOVA A., BERENSCHOT G., PUL C. V.: DTI visualization with streamsurfaces and evenly-spaced volume seeding. In *Data Visualization (Proc. of Eurographics/IEEE Symposium on Visualization)* (2004), Eurographics Association, pp. 173–182.

[vdB97] VAN DEN BERGEN G.: Efficient collision detection of complex deformable models using AABB trees. *Journal of Graphics Tools 2*, 4 (1997), 1–14.

[VHHFG05] VEGA-HIGUERA F., HASTREITER P., FAHLBUSCH R., GREINER G.: High performance volume splatting for visualization of neurovascular data. In *Proceedings of IEEE Visualization 2005* (2005).

[Vis07] VisiQuest, http://www.accusoft.com/products/visiquest/, 2007.

[VSC01] VASSILEV T., SPANLANG B., CHRYSANTHOU Y.: Fast cloth animation on walking avatars. *Computer Graphics Forum (Proc. of EUROGRAPHICS 2001) 20*, 3 (Sept. 2001), 260–267.

[VZKL06] VILANOVA A., ZHANG S., KINDLMANN G., LAIDLAW D.: *Visualization and Image Processing of Tensor Fields*. Springer Verlag series Mathematics and Visualization, 2006, ch. An Introduction to Visualization of Diffusion Tensor Imaging and its Applications, pp. 121–153.

[WEF*99] WIGSTRÖM L., EBBERS T., FYRENIUS A., KARLSSON M., ENGVALL J., WRANNE B., BOLGER A. F.: Particle trace visualization of intracardiac flow using time-resolved 3d phase contrast MRI. *Magnetic Resonance in Medicine 41*, 4 (1999), 793–799.

[Wer93] WERNECKE J.: *The Inventor Mentor: Programming Object-Oriented 3d Graphics with Open Inventor, Release 2*. Addison-Wesley Longman Publishing Co., Inc., Boston, MA, USA, 1993.

[WKL99] WEINSTEIN D., KINDLMANN G., LUNDBERG E.: Tensorlines: advectiondiffusion based propagation through diffusion tensor fields. In *Proc. of IEEE Visualization* (1999), pp. 249–253.

[WV05] WANG Z., VEMURI B.: DTI segmentation using an information theoretic tensor dissimilarity measure. *IEEE Transactions on Medical Imaging 24*, 10 (2005), 1267–1277.

[Zac98] ZACHMANN G.: Rapid collision detection by dynamically aligned DOP-trees. In *Proc. of IEEE Virtual Reality Annual International Symposium (VRAIS 1998)* (Atlanta, Georgia, Mar. 1998), pp. 90–97.

[Zac02] ZACHMANN G.: Minimal hierarchical collision detection. In *Proc. ACM Symposium on Virtual Reality Software and Technology (VRST 2002)* (Hong Kong, China, Nov. 2002), pp. 121–128.

[Zac07] ZACHMANN G. (Ed.):. *Proc. IEEE VR 2007 Workshop on 'Trends and Issues in Tracking for Virtual Environments'* (Charlotte, NC, USA, Mar.11 2007), IEEE, Shaker Verlag, Aachen, Germany.

[ZDK*01] ZHANG S., DEMIRALP Ç., KEEFE D., DASILVA M., GREENBERG B., BASSER P., PIERPAOLI C., CHIOCCA E., DEISBOECK T., LAIDLAW D.: An immersive virtual environment for DT-MRI volume visualization applications: a case study. In *IEEE Visualization* (October 2001), pp. 437–440.

[ZDL03] ZHANG S., DEMIRALP C., LAIDLAW D.: Visualizing diffusion tensor MR images using streamtubes and streamsurfaces. *IEEE Transactions on Visualization and Computer Graphics 9*, 4 (2003), 454–462.

[ZMB*03] ZHUKOV L., MUSETH K., BREEN D., WHITAKER R., BARR A.: Level set modeling and segmentation of dt-mri brain data. *J. Electronic Imaging 12*, 1 (2003), 125–133.

[ZY00] ZHANG D., YUEN M. M. F.: Collision detection for clothed human animation. In *Proceedings of the 8th Pacific Conference on Computer Graphics and Applications* (2000), IEEE Computer Society, pp. 328–337.